

# Solving the 2-Dimensional Fokker-Planck Equation for Strongly Correlated Neurons

Taşkın Deniz & Stefan Rotter

Bernstein Center Freiburg & Faculty of Biology,  
University of Freiburg, Hansastrasse 9a, 79104 Freiburg, Germany

(Dated: April 23, 2022)

Pairs of neurons in brain networks often share much of the input they receive from other neurons. Due to essential non-linearities of neuronal dynamics, the consequences for the correlation of the output spike trains are not well understood in the strongly correlated regime. Here we consider two leaky integrate-and-fire neurons with correlated white noise input. We analyze this scenario using a novel non-perturbative approach. Hence our treatment covers both weakly and strongly correlated dynamics, generalizing previous results based on linear response theory.

*Introduction.*—Both membrane potentials and action potentials recorded from nearby neurons in networks of the brain exhibit non-trivial statistical dependencies, typically quantified by cross correlation functions [1]. Theoretical models have emphasized that such correlations are an inevitable consequence if two neurons are part of the same network and share some synaptic input [2]. However, for non-linear neuron models, correlation functions are difficult to compute explicitly, especially for low firing rates in the strongly correlated regime [3, 4]. Previous analytical approaches have employed perturbation theory [5] to study pair correlations under the assumption of weak input correlation [6]. However, there is ample evidence of massive shared input for pairs of nearby neurons, resulting in strong correlations particularly of their membrane potentials [1]. A full theory of correlations, covering the case of both weak and strong shared input alike, demands non-perturbative methods that take non-linear effects into account [4]. In the work

presented here, we suggest a non-perturbative solution to the corresponding two-dimensional Fokker-Planck equation to describe correlated integrate-and-fire neurons in any regime, with arbitrary precision. We demonstrate that our theoretical predictions accurately fit to correlation functions computed from simulated spike trains.

*Model and Theory.*—We consider two leaky integrate-and-fire (LIF) model neurons receiving correlated inputs. Their dynamics are governed by the following stochastic differential equations

$$\tau_a \dot{V}_a = -V_a + \tau_a (\mu_a + \sigma_a [\sqrt{1-c} \xi_a \pm \sqrt{c} \xi_c]) \quad (1)$$

where input  $I_a = \mu_a + \sigma_a [\sqrt{1-c} \xi_a \pm \sqrt{c} \xi_c]$  with private white noise  $\xi_a$  ( $a = 1, 2$ ) and shared white noise  $\xi_c$ , all components being independent. Input correlation coefficient is given as  $\pm c$ , where  $0 \leq c < 1$  and  $\tau_a, \mu_a$  and  $\sigma_a$  are constant parameters characterizing both the neuron model and the input. Without loss of generality we take only the positive sign in  $\pm \sqrt{c}$ . The corresponding Fokker-Planck equation is

$$\frac{\partial P}{\partial t} = \partial_1 \left( \left( \frac{V_1}{\tau_1} - \mu_1 \right) P \right) + \partial_2 \left( \left( \frac{V_2}{\tau_2} - \mu_2 \right) P \right) + \frac{1}{2} (\partial_1 \ \partial_2) \begin{pmatrix} \sigma_1^2 & c\sigma_1\sigma_2 \\ c\sigma_1\sigma_2 & \sigma_2^2 \end{pmatrix} \begin{pmatrix} \partial_1 \\ \partial_2 \end{pmatrix} P \quad (2)$$

where we define  $\partial_a \equiv \frac{\partial}{\partial V_a}$  and  $P \equiv P(V_1, V_2, t)$ . Using the new variables  $x = \frac{V_1 - \mu_1 \tau_1}{\sigma_1 \sqrt{\tau_1}}$  and  $y = \frac{V_2 - \mu_2 \tau_2}{\sigma_2 \sqrt{\tau_2}}$  the equation can be rewritten as

$$\frac{\partial P}{\partial t} = \frac{1}{\tau_1} \mathcal{L}_1 P + \frac{1}{\tau_2} \mathcal{L}_2 P + \frac{c}{\sqrt{\tau_1 \tau_2}} \mathcal{L}_{12} P \quad (3)$$

$$\mathcal{L}_1 P = \frac{\partial(xP)}{\partial x} + \frac{1}{2} \frac{\partial^2 P}{\partial x^2} \quad (4)$$

$$\mathcal{L}_2 P = \frac{\partial(yP)}{\partial y} + \frac{1}{2} \frac{\partial^2 P}{\partial y^2} \quad (5)$$

$$\mathcal{L}_{12} = \frac{\partial^2 P}{\partial x \partial y}. \quad (6)$$

The first two terms represent independent populations, and they fully describe the 2D dynamics for  $c = 0$ . The

third term represents the correlated diffusion for  $c > 0$ .

In order to calculate the cross-covariance function of output spike trains, we first compute the joint steady state distribution of membrane potentials from  $\frac{\partial P}{\partial t} = 0$ . We have threshold potentials  $x_t, y_t$ , reset potentials  $x_r, y_r$  and boundary conditions

$$P_0(x, y_t) = 0 = P_0(x_t, y) \quad (7a)$$

$$P_0(x, -\infty) = 0 = P_0(-\infty, y) \quad (7b)$$

$$\partial_x P_0(x_r - \epsilon, y) - \partial_x P_0(x_r + \epsilon, y) \stackrel{\epsilon \rightarrow 0}{=} \partial_x P_0(x_t, y) \quad (7c)$$

$$\partial_y P_0(x, y_r - \epsilon) - \partial_y P_0(x, y_r + \epsilon) \stackrel{\epsilon \rightarrow 0}{=} \partial_x P_0(x, y_t) \quad (7d)$$

We derive an expansion of the stationary equation in terms of eigenfunctions of the uncoupled operators ([7])

$$\mathcal{L}_1 f_i = \lambda_{1i} f_i, \quad \mathcal{L}_2 g_i = \lambda_{2i} g_i \quad (8)$$

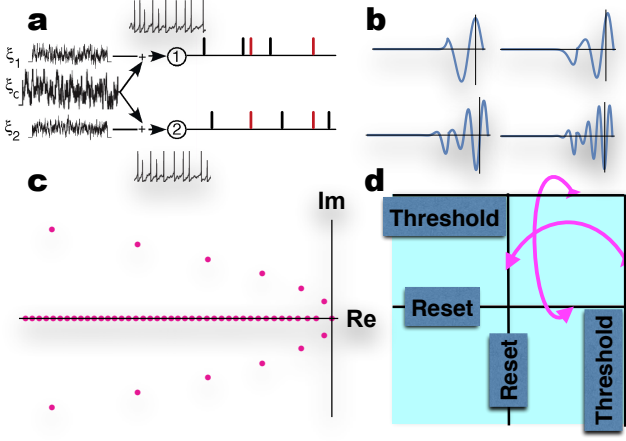


FIG. 1. (a) Leaky integrate-and-fire neurons driven by strong shared noise, inducing synchronicity in the output spike trains. (b) Examples of eigenfunctions with increasing  $|\text{Re}(\lambda)|$ . (c) A typical discrete eigenvalue spectrum of the diffusion-based LIF model, comprising both real and complex conjugate pairs of eigenvalues with  $\text{Re}(\lambda) \leq 0$ . (d) Boundary conditions in 2D voltage space with threshold potentials  $x_t, y_t$  and resting potentials  $x_r, y_r$ . The magenta arrows represent the reset mechanism once the threshold was hit and a spike was elicited in either neuron.

with boundary conditions given as

$$f_i(x_t) = 0 = \lim_{x \rightarrow -\infty} f_i(x) \quad (9)$$

$$\partial_x f_i(x_t) \stackrel{\epsilon \rightarrow 0}{=} \partial_x f_i(x_r - \epsilon) - \partial_x f_i(x_r + \epsilon). \quad (10)$$

Analogous expressions hold for  $g_i(y)$ . The eigenvalue spectrum of this problem is countable with both real and pairs of complex conjugate eigenvalues (Fig. 1c). (We assume here that the index  $i$  increases with  $|\text{Re}(\lambda_i)|$ .) In order to expand the solution in the eigenspace of a non-selfadjoint differential operator, the dual eigenvalue problem needs to be solved as well (see [7] for details.)

$$\mathcal{L}_1^\dagger \tilde{f}_i = \lambda_{1i} \tilde{f}_i, \quad \mathcal{L}_2^\dagger \tilde{g}_i = \lambda_{2i} \tilde{g}_i \quad (11)$$

with conjugate boundary conditions

$$\tilde{f}_i(x_t) = \tilde{f}_i(x_r), \quad \tilde{g}_i(y_t) = \tilde{g}_i(y_r). \quad (12)$$

This guarantees that the basis  $\{f_i\}$  and the conjugate basis  $\{\tilde{f}_i\}$  are bi-orthogonal in Hilbert Space

$$\int_{-\infty}^{x_t} \tilde{f}_i(x) f_j(x) dx = \delta_{ij} \quad (13)$$

where we select free coefficients to satisfy bi-orthonormality. The solution to Eq. 3 can now be expanded in terms of functions that individually satisfy the boundary conditions Eq. 7

$$P_0(x, y) = f_0(x)g_0(y) + F(x)SG(y) \quad (14)$$

where we define  $F(x)SG(y) \equiv \sum_{ij} S_{ij} f_i(x)g_j(y)$ , for some coefficients  $S_{ij} \in \mathbb{C}$ . This expansion exactly satisfies the constraints for marginal distributions

$$\int_{-\infty}^{y_t} P_0(x, y) dy = f_0(x), \quad \int_{-\infty}^{x_t} P_0(x, y) dx = g_0(y) \quad (15)$$

where the probability density function  $f_0$  is given by

$$f_0(x) = 2r_1\tau_1 e^{-x^2} \int_x^{x_t} \Theta(u - x_r) e^{u^2} du, \quad (16)$$

where  $\Theta(x)$  is the Heaviside step function. The density  $g_0(y)$  is defined analogously. Steady state firing rates of both neurons are given by

$$r_1 = \frac{1}{\tau_1} \left[ \int_0^\infty e^{-u^2} \frac{e^{x_t u} - e^{x_r u}}{u} du \right]^{-1} \quad (17)$$

and a similar expression for  $r_2$ . Using Eq. 8, the solution can now implicitly be written in terms of eigenfunctions

$$F(x)\Lambda_1 S G(y) + F(x)S\Lambda_2 G(y) + \tilde{c} \partial_x F(x) S \partial_y G(y) = -\tilde{c} \partial_x f_0(x) \partial_y g_0(y) \quad (18)$$

with diagonal matrix  $\Lambda_{a,ij} = \frac{\lambda_{ai} \delta_{ij}}{\tau_a}$  and constant  $\tilde{c} = \frac{c}{\sqrt{\tau_1 \tau_2}}$ . In order to actually solve Eq. 18 we express the action of the derivative operators on the eigenbasis as

$$X_{ij} = \int_{-\infty}^{x_t} \tilde{f}_i(x) \partial_x f_j(x) dx \quad (19)$$

and similarly for  $Y$ . The final equation in matrix form is

$$\Lambda_1 S + S\Lambda_2 + \tilde{c} X^T S Y = -\tilde{c} X_0 \otimes Y_0. \quad (20)$$

*Spike Train Correlations.*—The covariance function of two stationary spike trains  $\mathbb{S}_a(t) = \sum_l \delta(t - t_l^a)$  ( $a = 1, 2$ ) is given as

$$C_{12}(\tau) = \langle \mathbb{S}_1(t) \mathbb{S}_2(t+\tau) \rangle - \langle \mathbb{S}_1(t) \rangle \langle \mathbb{S}_2(t) \rangle \quad (21)$$

where  $\langle \mathbb{S}_a(t) \rangle = r_a$ , with  $\langle \cdot \rangle$  indicating the ensemble average. Using renewal theory, it can be expressed in terms of the conditional firing rate  $r_{1|2}(\tau)$  as

$$C_{12}(\tau) = r_2(r_{1|2}(\tau) - r_1). \quad (22)$$

We derive the conditional firing rate from the stationary joint membrane potential distribution  $P_0(x, y)$  via the distribution of the membrane potential conditional to a spike at  $t_0 = 0$  found as  $P_{1|2}(x) = -\frac{1}{2r_2\tau_2} \partial_y P_0(x, y_t)$ , since  $\int_{-\infty}^{x_t} \partial_y P_0(x, y_t) dx = -2r_2\tau_2$  by construction. Therefore, we have to solve the initial value problem

$$f(t_0, x) = -\frac{1}{2r_2\tau_2} \partial_y P_0(x, y_t) \quad (23)$$

$$\tau_1 \partial_t f = \mathcal{L}_1 f \quad (24)$$

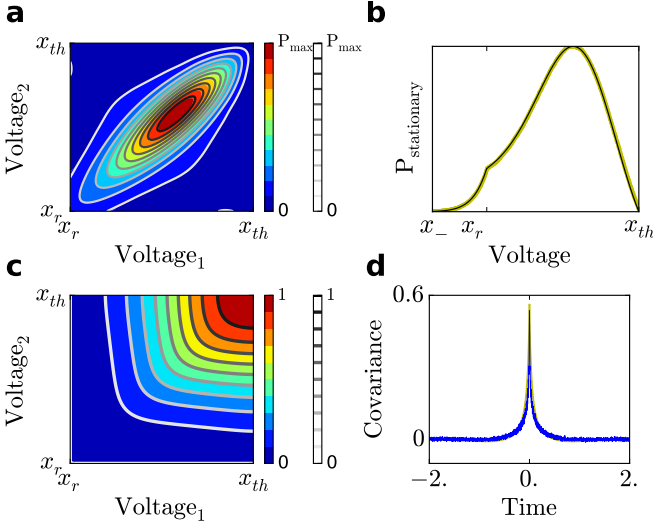


FIG. 2. Simulations and theory yield practically identical results, demonstrated here for  $x_r = y_r = -2.0$ ,  $x_t = y_t = 0.8$  and  $c = 0.9$ . (a) Joint membrane potential distribution of simulated data (smoothed 2D histogram of simultaneously recorded membrane potentials), compared to  $P_0(x, y)$ , Eq. 18. The  $L_1$  error is approx. 0.02, partially caused by a boundary effect for discrete-time simulations of Eq. 1. (b) Marginal distribution  $f_0(x)$ , Eq. 16 (black: data, yellow: theory). (c) Same as (a), comparison between cumulative distributions  $\int_{-\infty}^x \int_{-\infty}^y P_0(x, y) dx dy$ . (d) Symmetric correlation function  $C_{12}(\tau)$  with time rescaled by  $\tau_1$ . The blue curve is the covariance function of simulated spike trains, while the yellow curve is a numerical rendering of the theory developed here.

where  $\mathcal{L}_1$  is the time evolution operator in Eq. 8. The instantaneous conditional rate in Eq. 22 is then  $r_{1|2}(t) = -\frac{1}{2\tau_1} \partial_x f(x, t)$ . The instantaneous conditional distribution is given by

$$f(x, t) = f_0(x) + \frac{1}{2r_2\tau_2} \sum_i \left( \sum_j S_{ij} \right) e^{\lambda_{1i}t/\tau_1} f_i(x). \quad (25)$$

The exit flux at threshold  $r_{1|2}(t)$  inserted into Eq. 22 yields the covariance function

$$C_{12}(\tau) = \frac{1}{4\tau_1\tau_2} \sum_{ij} [\Theta(\tau)e^{\Lambda_1\tau}S + \Theta(-\tau)Se^{-\Lambda_2\tau}]_{ij} \quad (26)$$

for  $\tau = t_1 - t_2$  and  $\Lambda_{a,ij} = \frac{\lambda_{ai}\delta_{ij}}{\tau_a}$ . Using the symmetry  $C_{12}(\tau) = C_{21}(-\tau)$  we obtain the covariance function for negative time lags as well. The correlation coefficient as considered in [6] is computed as (see [7] for details)

$$C_{out}(c) = \frac{-\tilde{c}}{4CV_1CV_2\sqrt{r_1r_2}} \sum_{ij} \frac{(XS Y + X_0 Y_0)_{ij}}{\Lambda_{1,i}\Lambda_{2,j}} \quad (27)$$

with  $CV_a$  being the coefficients of variation of the two output spike trains. Here one can see how the correlation transfer depends non-linearly on  $c$  as  $S$  is a non-linear function of  $c$ .

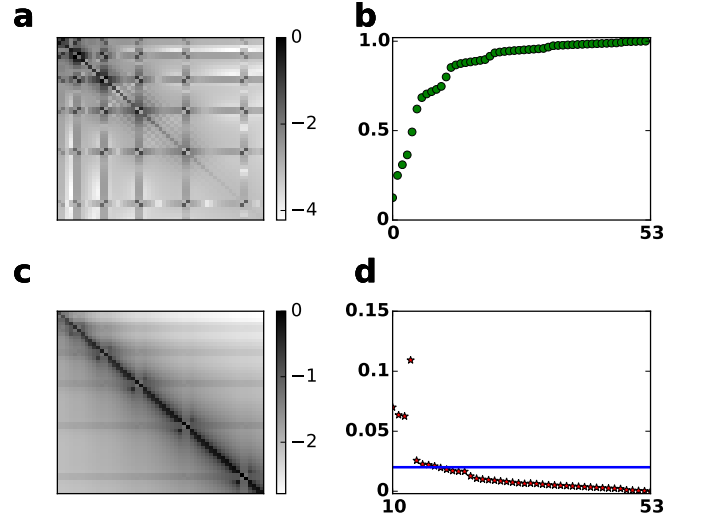


FIG. 3. Numerical example solution with  $x_r = y_r = -2.0$ ,  $x_t = y_t = 0.8$  and  $c = 0.9$ . (a) logarithmic rendering  $\log_{10}(|S_{ij}|/\max(|S_{ij}|))$  of mode coupling matrix  $S$  (size:  $53 \times 53$ ). (b) Relative convergence of correlation coefficients  $C_n^{(rel)} = \sum_{j=1}^n \sum_i (S\Lambda^{-1})_{ij} / \sum_{ij} (S\Lambda^{-1})_{ij}$ , in Eq. 27. (c) Matrix representation  $X$  of the derivative operators presented as in (a). (d) Relative error  $\int_{-\infty}^{x_r} \int_{-\infty}^{y_r} dx dy |P_0^N(x, y) - P_0^{(n)}(x, y)|$ , where  $n$  is truncation number and  $N = 53$  is the maximum truncation number in Eq. 14.  $N$  is the number of eigenvalues with property  $|Re(\lambda_i)| < 100$ . Here we solved Eq. 20 for different  $n$ . The blue line is the  $L_1$  error in Fig. 2a.

*Relation to Perturbative Approaches.*—The perturbative solution for small  $c$  is  $S = S_0 + cS_1 + c^2S_2 + \dots$ . Inserting this into Eq. 20 we obtain

$$\tilde{c}X(S_0 + cS_1 + c^2S_2 + \dots)Y + \Lambda_1(S_0 + cS_1 + \dots) + (S_0 + cS_1 + \dots)\Lambda_2 = -\tilde{c}X_0Y_0. \quad (28)$$

We find that  $S_0 = 0$  for  $c = 0$ , since  $\Lambda_{1k}S_{0,kl} + \Lambda_{2l}S_{0,kl} = 0$  has no nonzero solution with  $\lambda_{1k} \neq -\lambda_{2k}$ , except  $\lambda_{1k} = 0 = \lambda_{2k}$  in which case we have set the coefficient of  $f_{0g_0}$  to 1. The  $O(c)$  equation for  $S_1$  is

$$\Lambda_1S_1 + S_1\Lambda_2 = -\frac{1}{\sqrt{\tau_1\tau_2}}X_0 \otimes Y_0 \quad (29)$$

and using the definition  $\psi_{kl} \equiv \frac{\sqrt{\tau_1\tau_2}}{\lambda_{1k}\tau_2 + \lambda_{2l}\tau_1}$  the solution is

$$S_{1,kl} = -\psi_{kl}X_{0,k}Y_{0,l}. \quad (30)$$

The recursion relation for terms of order  $O(c^n)$  is  $S_{n,kl} = -\psi_{kl} \sum_{ij} X_{ki}Y_{lj}S_{n-1,ij}$  with which one can expand the full perturbative series. Instead, for the non-perturbative regime,  $S$  is obtained by solving a tensor equation

$$\sum_{kl} M_{ijkl}S_{kl} = F_{ij} \quad (31)$$

$$M_{ijkl} = \tilde{c}X_{ik}Y_{jl} + (\Lambda_{1i} + \Lambda_{2j})\delta_{ik}\delta_{jl} \quad (32)$$

$$F_{ij} = -\tilde{c}X_{0,i}Y_{0,j} \quad (33)$$

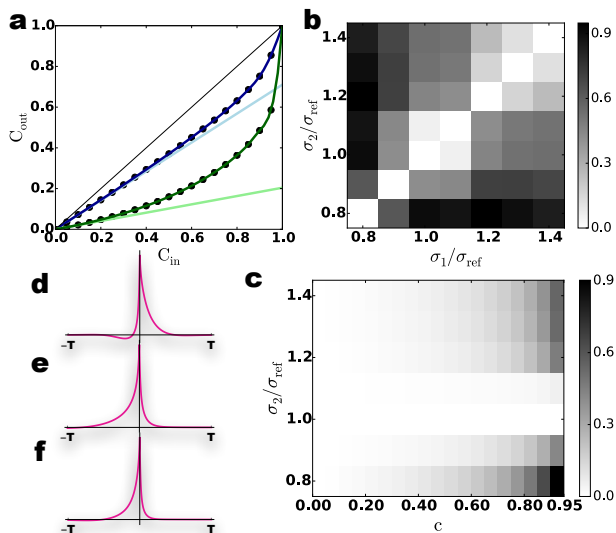


FIG. 4. Heterogeneous parameters lead to nonsymmetric cross-correlation functions. (a) Non-perturbative correlation transfer functions  $C_{out}(C_{in})$  in Eq. 27 for symmetric parameters and for high and low firing rates, respectively (blue:  $r_b = \frac{0.231}{\tau_1}$ ,  $CV^2 = 0.5$ ; green:  $r_g = \frac{0.017}{\tau_1}$ ,  $CV^2 = 0.98$ ). Slopes of light blue and light green lines (corresponding to  $\frac{dC_{out}}{dC_{in}}$  at  $C_{in} = 0$ ), are computed using perturbation theory as in [6]. (b) Asymmetry of the cross-covariance function  $\mathcal{A} = \int_0^\infty d\tau |C_{21}(\tau) - C_{21}(-\tau)|$  for two different input variances  $\sigma_1$  vs.  $\sigma_2$ , for  $c = 0.9$ . (c)  $\mathcal{A}$  for changing input variance  $\sigma_2$ , fixed  $\sigma_1 = \sigma_{ref}$  and different values of  $c$  between 0 and 0.95. Examples of asymmetric cross covariance functions (time rescaled with  $\tau_1$  as in Fig. 2d,  $c = 0.9$ , time window  $T = 2$ ) for heterogenous parameters in Eq. 2 : (d) asymmetric mean input  $\mu_a$ , (e) asymmetric membrane time constant  $\tau_a$ , (f) asymmetric input variance  $\sigma_a^2$ .

which can be obtained by flattening indices and using conventional linear algebra techniques (Fig. 3a).

*Asymmetric Correlations.*—Neurons in biological networks have widely distributed parameters, and this heterogeneity may also influence information processing [8]. Moreover, robust asymmetries in spike correlations could lead to asymmetric synaptic efficacies when integrated via linear spike timing dependent plasticity [9]. Our approach reveals a temporal asymmetry in covariance functions, Eq. 26 related to a heterogeneity of intrinsic neuron parameters and input parameters (Fig. 4b). Such temporal asymmetry is more pronounced for large values of  $c$ , especially in the non-perturbative regime that we address in this work (Fig. 4b–f). (See [7] for parameters.)

*Discussion and Conclusions.*—We developed a novel theory of correlation functions for two LIF model neurons driven by shared input. Our approach can deal with the full range of input correlations  $0 \leq c < 1$ , and the expansion converges fast (Fig. 3b,d). Also, our method is widely generalizable [3]. Low output firing rates generally require a non-perturbative treatment, while the

approximation derived from linear response theory [6] is reasonably precise if firing rates are high (Fig. 4a). We considered firing rates between 1 and 25 Hz, and values for  $CV^2$  between 0.5 and 1, consistent with what is reported in neocortical neurons *in vivo*. Strong correlations of membrane potentials were observed in nearby neurons of cortical networks [1], compatible with the high degree of shared input suggested from neuroanatomical studies. In the strongly correlated regime the correlation transfer function is non-linear [4, 6] and the dynamics is quite sensitive to heterogeneities of the input and of the model parameters [8]. Recent experiments demonstrated that asymmetric correlation functions arise in neocortical neurons as well [8]. Correlation asymmetries could make an important contribution to structure formation in networks through Hebbian learning on short time scales in the range of the membrane time constant of neurons [9].

*Acknowledgements.*—We thank Man-Yi Yim for discussions. Funding by the BMBF (grant BFNT 01GQ0830) and the DFG (grant EXC 1086) is gratefully acknowledged.

- 
- [1] I. Lampl, I. Reichova, and D. Ferster, *Neuron* **22**, 361 (1999); M. Okun and I. Lampl, *Nature Neuroscience* **11**, 535 (2008); J. F. Poulet and C. C. Petersen, *Nature* **454**, 881 (2008).
  - [2] S. Ostojic, N. Brunel, and V. Hakim, *J Neurosci* **29**, 10234 (2009); V. Pernice, B. Staude, S. Cardanobile, and S. Rotter, *PLoS Computational Biology* **7** (2011), 10.1371/journal.pcbi.1002059; *Physical Review E - Statistical, Nonlinear, and Soft Matter Physics* **85**, 1 (2012), arXiv:arXiv:1201.0288v2.
  - [3] R. Rosenbaum, F. Marpeau, J. Ma, A. Barua, and K. Josić, *Journal of Mathematical Biology* **65**, 1 (2012), arXiv:1011.0669.
  - [4] M. Schultze-Kraft, M. Diesmann, S. Grün, and M. Hellas, *PLoS Computational Biology* **9**, e1002904 (2013), arXiv:1207.7228.
  - [5] N. Brunel and V. Hakim, *Neural Computation* **11**, 1621 (1999), arXiv:9904278 [cond-mat]; B. Lindner and L. Schimansky-Geier, *Physical Review Letters* **86**, 2934 (2001).
  - [6] J. de la Rocha, B. Doiron, E. Shea-Brown, K. Josić, and A. Reyes, *Nature* **448**, 802 (2007); E. Shea-Brown, K. Josić, J. de la Rocha, and B. Doiron, *Physical Review Letters* **100**, 108102 (2008).
  - [7] Supplementary material.
  - [8] M. Y. Yim, A. Aertsen, and S. Rotter, *Physical Review E - Statistical, Nonlinear, and Soft Matter Physics* **87**, 1 (2013), arXiv:1208.5350; M. Y. Yim, J. Wolfart, A. Aertsen, and S. Rotter, *Frontiers in Computational Neuroscience* **6** (2012), 10.3389/conf.fncom.2012.55.00030; K. Padmanabhan and N. N. Urban, *Nature Neuroscience* **13**, 1276 (2010).
  - [9] A. Morrison, M. Diesmann, and W. Gerstner, *Biological Cybernetics* **98**, 459 (2008); B. Babadi and L. F. Abbott, *PLoS Computational Biology* **9**, e1002906 (2013)

# Supplementary Material: Solving the 2-Dimensional Fokker-Planck Equation for Strongly Correlated Neurons

## Introduction

In this appendix, we provide the essential details of our computations. First, we show how one derives the spectrum and respective dual-spectrum for non-adjoint operators. Second, we compare our non-perturbative method to the classical perturbation theory derived in [S5], and used in [S6]. Third, we prove all results presented in the main text. Fourth, we show how the 2D equation is derived from the Kolmogorov forward equation as a simple generalization of the 1D case. Finally, we explain numerical procedures and data analysis methods that were used to compare of the theoretical functions with functions obtained from simulated data.

## Appendix A: Eigenvalue spectrum of 1D operators

Two independent solutions of the following Sturm-Liouville problem

$$\mathcal{L}_1\phi = \frac{\partial(x\phi)}{\partial x} + \frac{1}{2} \frac{\partial^2\phi}{\partial x^2} = \lambda\phi \quad (\text{S1})$$

are given in [S12] as

$$\phi_1(x, \lambda) = {}_1F_1\left(\frac{1-\lambda}{2}, 1/2, -x^2\right) \quad (\text{S2})$$

$$\phi_2(x, \lambda) = \frac{\Gamma(\frac{\lambda}{2})}{\Gamma(\frac{\lambda+1}{2})} {}_1F_1\left(\frac{1-\lambda}{2}, \frac{1}{2}, -x^2\right) + 2x {}_1F_1\left(1 - \frac{\lambda}{2}, \frac{3}{2}, -x^2\right) \quad (\text{S3})$$

where  ${}_1F_1(a, b, z)$  is the Confluent Hypergeometric Function of the first kind [S12]. We note that the fraction  $\frac{\Gamma(\frac{\lambda}{2})}{\Gamma(\frac{\lambda+1}{2})}$  is regularized, as the reciprocal of gamma functions can be analytically continued to zero at its poles [S12].

There is another basis which is known to be numerically more stable and given in terms of Parabolic Cylinder Functions as [S5]

$$\psi_1(x, \lambda) = e^{-\frac{x^2}{2}} D_{-\lambda}(x/\sqrt{2}) \quad (\text{S4})$$

$$\psi_2(x, \lambda) = e^{-\frac{x^2}{2}} D_{\lambda-1}(ix/\sqrt{2}) \quad (\text{S5})$$

and we will discuss them in the following sections. All in all, it doesn't matter which basis is used to expand a function in the eigenspace of  $\mathcal{L}_1$ . Eigenfunctions are unique up to some normalization condition which we select to be  $R(\lambda) = -\frac{1}{2}\partial_x f(\lambda, x_t) = 1$ .

The eigenvalue spectrum of Eq. S1 is discrete and can be found by satisfying the boundary conditions

$$\begin{aligned} f_\lambda(x_t) = 0 &= \lim_{x \rightarrow -\infty} f_\lambda(x) \\ f_\lambda(x_r - \epsilon) &\stackrel{\epsilon \rightarrow 0}{=} f_\lambda(x_r + \epsilon) \\ \partial_x f_\lambda(x_t) &\stackrel{\epsilon \rightarrow 0}{=} \partial_x f_\lambda(x_r - \epsilon) - \partial_x f_\lambda(x_r + \epsilon). \end{aligned} \quad (\text{S6})$$

A general family of solutions with the property  $\lim_{x \rightarrow -\infty} f_\lambda(x) = 0$  is given as

$$f_\lambda(x) = \begin{cases} a(\lambda)\phi_1(\lambda, x) + b(\lambda)\phi_2(\lambda, x) & x_r \leq x < x_t \\ d(\lambda)\phi_2(\lambda, x) & x_r \geq x \end{cases}.$$

The boundary conditions Eq.S32 require

$$\begin{aligned} a(\lambda)\phi_1(\lambda, x_t) + b(\lambda)\phi_2(\lambda, x_t) &= 0 \\ a(\lambda)\phi_1(\lambda, x_r) + b(\lambda)\phi_2(\lambda, x_r) - d(\lambda)\phi_2(\lambda, x_r) &= 0 \\ a(\lambda)(\phi_1'(\lambda, x_r) - \phi_1'(\lambda, x_t)) + b(\lambda)(\phi_2'(\lambda, x_r) - \phi_2'(\lambda, x_t)) - d(\lambda)\phi_2'(\lambda, x_r) &= 0. \end{aligned}$$

In order to have non-zero solutions the determinant of the coefficient matrix must satisfy

$$\begin{vmatrix} \phi_1(\lambda, x_t) & \phi_2(\lambda, x_t) & 0 \\ \phi_1(\lambda, x_r) & \phi_2(\lambda, x_r) & -\phi_2(\lambda, x_r) \\ (\phi_1'(\lambda, x_r) - \phi_1'(\lambda, x_t)) & (\phi_2'(\lambda, x_r) - \phi_2'(\lambda, x_t)) & -\phi_2'(\lambda, x_r) \end{vmatrix} = 0. \quad (\text{S7})$$

The eigenvalues  $\{\lambda_i\}$  are countably many isolated points given as solutions of

$$\phi_2(\lambda, x_t) / Wr(x_t) - \phi_2(\lambda, x_r) / Wr(x_r) = 0 \quad (\text{S8})$$

where we have the Wronskian  $Wr(x) = \phi_1'(x)\phi_2(x) - \phi_1(x)\phi_2'(x) = 2e^{-x^2}$ . The spectrum is the same as given in [S5]. In order to find  $a$  and  $b$ , we need to fix  $d(\lambda)$

$$a(\lambda) = \frac{\phi_2(\lambda, x_r)e^{x_r^2} d(\lambda)}{e^{x_r^2}\phi_1(\lambda, x_r) - e^{x_t^2}\phi_1(\lambda, x_t)}$$

$$b(\lambda) = \frac{-\phi_1(\lambda, x_t)e^{x_t^2} d(\lambda)}{e^{x_r^2}\phi_1(\lambda, x_r) - e^{x_t^2}\phi_1(\lambda, x_t)}.$$

We can find the exit rate at threshold  $R(\lambda)$  as

$$\begin{aligned} R(\lambda) &= -\frac{1}{2}\partial_x f(\lambda, x_t) = -\frac{1}{2}(a(\lambda)\phi_1'(\lambda, x_t) + b(\lambda)\phi_2'(\lambda, x_t)) \\ &= -\frac{1}{2}d(\lambda) \frac{\phi_2(\lambda, x_r)\phi_1'(\lambda, x_t)e^{x_r^2} - \phi_2'(\lambda, x_t)\phi_1(\lambda, x_t)e^{x_t^2}}{e^{x_r^2}\phi_1(\lambda, x_r) - e^{x_t^2}\phi_1(\lambda, x_t)} \\ &= -\frac{1}{2}d(\lambda) \frac{\phi_2(\lambda, x_t)\phi_1'(\lambda, x_t)e^{x_t^2} - \phi_2'(\lambda, x_t)\phi_1(\lambda, x_t)e^{x_t^2}}{e^{x_r^2}\phi_1(\lambda, x_r) - e^{x_t^2}\phi_1(\lambda, x_t)} \\ &= -\frac{1}{2}d(\lambda) \frac{e^{x_t^2}(\phi_2(\lambda, x_t)\phi_1'(\lambda, x_t) - \phi_2'(\lambda, x_t)\phi_1(\lambda, x_t))}{e^{x_r^2}\phi_1(\lambda, x_r) - e^{x_t^2}\phi_1(\lambda, x_t)} \\ &= -\frac{1}{2}d(\lambda) \frac{-e^{x_t^2} 2e^{-x_t^2}}{e^{x_r^2}\phi_1(\lambda, x_r) - e^{x_t^2}\phi_1(\lambda, x_t)} \\ &= \frac{d(\lambda)}{e^{x_r^2}\phi_1(\lambda, x_r) - e^{x_t^2}\phi_1(\lambda, x_t)} \end{aligned}$$

where we select

$$d(\lambda) = e^{x_r^2}\phi_1(\lambda, x_r) - e^{x_t^2}\phi_1(\lambda, x_t) \quad (\text{S9})$$

in order to have  $R(\lambda) = 1$ . As a result we obtain

$$a(\lambda) = \phi_2(\lambda, x_r)e^{x_r^2} \quad \text{and} \quad b(\lambda) = -\phi_1(\lambda, x_t)e^{x_t^2}. \quad (\text{S10})$$

We note that there is a numerical method which generalizes the procedure above to neuron models with no known explicit solutions [S13].

## Appendix B: Dual eigenspace

In this section we explain non-orthogonal projections to a non-adjoint operator eigenspace. The solution to the Sturm-Liouville equation,  $f(\lambda, x)$ , satisfying

$$\mathcal{L}_1 f = \frac{\partial(xf)}{\partial x} + \frac{1}{2} \frac{\partial^2 f}{\partial x^2} = \lambda f \quad (\text{S11})$$

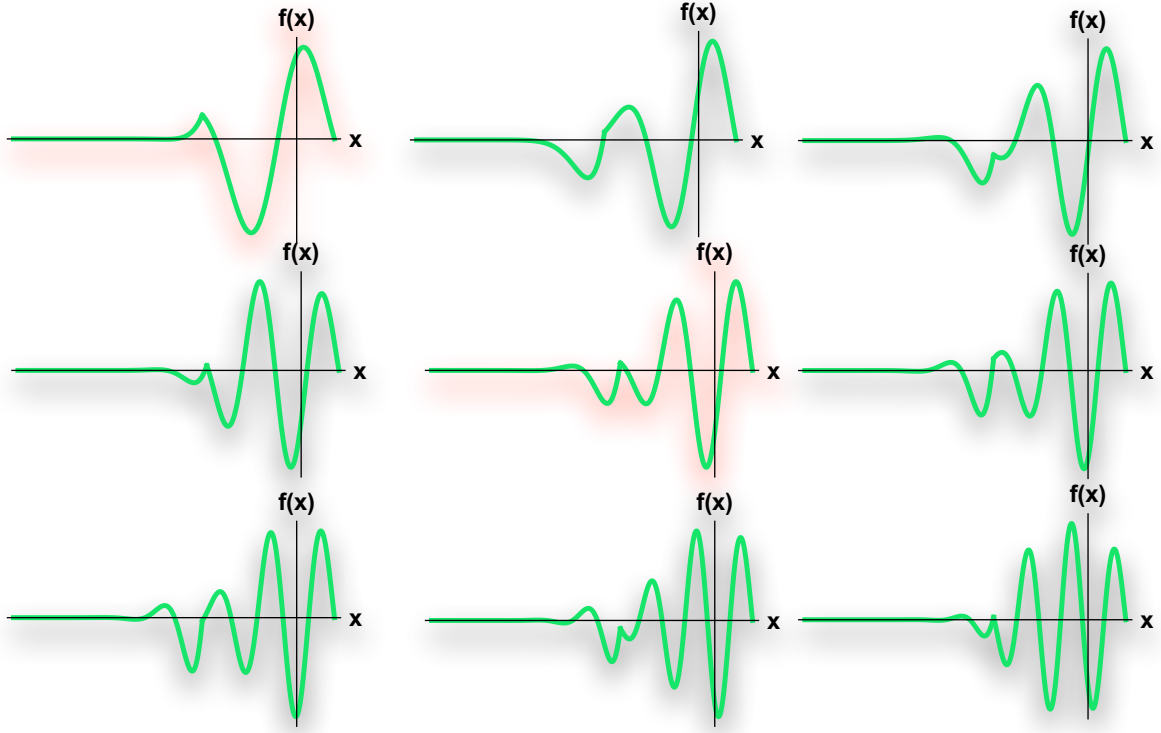


FIG. S1. Eigenvectors for  $y_\theta = 0.8$  and  $y_r = -2.$ , which corresponds to typical values in the fluctuation driven regime. Grey shaded eigenvectors belong to real eigenvalues, and red shaded curves are the real part of eigenvectors that belong to complex (non-real) eigenvalues.

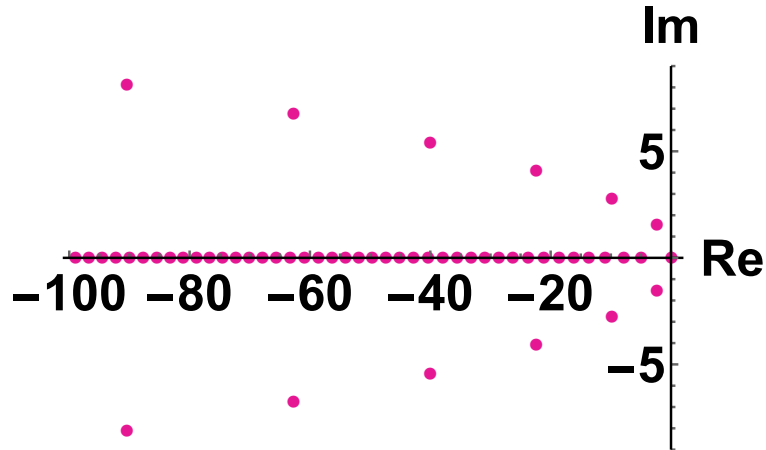


FIG. S2. Eigenvalue spectrum for  $y_\theta = 0.8$  and  $y_r = -2.$ , which corresponds to typical values in fluctuation driven regime. The eigenvalue  $\lambda_0 = 0$  does not appear in the correlation expansion.

are given above. As  $\mathcal{L}_1$  is not an adjoint operator (because of reset boundary conditions in Eq. S6), in order to build a bi-orthogonal basis, we need to find the dual equation  $\mathcal{L}^\dagger f = \lambda f$  [S14]

$$\langle \tilde{f}_j \mathcal{L}_1^\dagger f_i \rangle - \langle \tilde{f}_j, \mathcal{L}_1 f_i \rangle = (\lambda_j - \lambda_i) \langle f_i, \tilde{f}_j \rangle \quad (\text{S12})$$

where  $\langle \cdot, \cdot \rangle$  is an inner product in Hilbert space which is given in [S14] explicitly as

$$\int dx f_i \mathcal{L}_1^\dagger \tilde{f}_j - \int dx \tilde{f}_j \mathcal{L}_1 f_i = (\lambda_j - \lambda_i) \int dx f_i \tilde{f}_j. \quad (\text{S13})$$

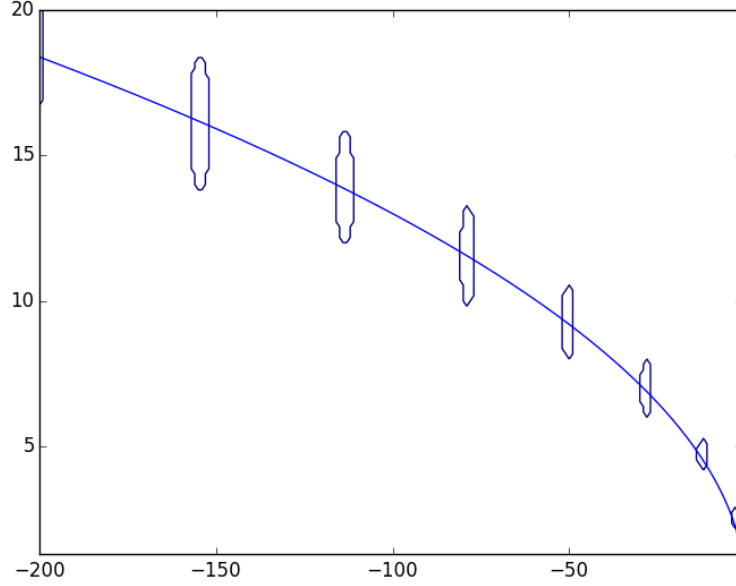


FIG. S3. We observe that the imaginary poles approximately satisfy  $\text{Im}(\lambda)^2 \propto \text{Re}(\lambda)$  with  $\text{Re}(\lambda_n) \sim (2n-1)^2$  asymptotically. Complex conjugate of this curve has the same property, because eigenvalues are in complex conjugate pairs. Enclosed by the dark blue curves are all complex numbers, where the spectral function satisfies  $|f_{\text{spec}}(\lambda)| < \epsilon$  for a given  $\epsilon > 0$ . We note that imaginary eigenvalues are absent for values  $V_{th} \ll \mu$ .

Here the LHS is the surface term which can be simplified by integration by parts as

$$(\lambda_j - \lambda_i) \int dx f_i \tilde{f}_j = -[\tilde{f}_j J_j]_{-\infty}^{x_r} - [\tilde{f}_j J_j]_{x_r}^{x_t} - [\partial_x \tilde{f}_j f_j]_{-\infty}^{x_t} \quad (\text{S14})$$

where we defined  $J_i \equiv -x f_i - \frac{1}{2} \partial_x f_i$  and  $[f(x)]_b^a \equiv f(a) - f(b)$ . Dual boundary conditions that satisfy zero surface term are then

$$\tilde{f}(x_r) = \tilde{f}(x_t). \quad (\text{S15})$$

This guarantees that  $\langle f_i, \tilde{f}_j \rangle = \delta_{ij}$  with appropriate choice of constants. The corresponding dual equation is

$$\mathcal{L}_1^\dagger \tilde{f} = -x \frac{\partial \tilde{f}}{\partial x} + \frac{1}{2} \frac{\partial^2 \tilde{f}}{\partial x^2}. \quad (\text{S16})$$

The transformation  $\tilde{f}_i = e^{x^2} h(x)$  with following relations

$$\begin{aligned} \tilde{f}' &= (2xh + h') e^{x^2} \\ \tilde{f}'' &= ((2 + 4x^2)h + 4xh' + h'') e^{x^2} \\ -x\tilde{f}' &= (-2x^2h - xh') e^{x^2} \end{aligned}$$

with  $\tilde{f}_i$  satisfying Eq. S16 for an eigenvalue  $\lambda_i$ . It can be shown after insertion of equations above in Eq. S16 that

$$\mathcal{L}_1 h = \frac{\partial(xh)}{\partial x} + \frac{1}{2} \frac{\partial^2 h}{\partial x^2} = \lambda h \quad (\text{S17})$$

holds. The dual eigenfunctions are found to be

$$\tilde{f}(\lambda, x) = e^{x^2} (\tilde{a}(\lambda) \phi_1(\lambda, x) + \tilde{b}(\lambda) \phi_2(\lambda, x)). \quad (\text{S18})$$



The boundary conditions require that continuous and differentiable solutions satisfy

$$e^{x_r^2}(\tilde{a}(\lambda)\phi_1(\lambda, x_r) + \tilde{b}(\lambda)\phi_2(\lambda, x_r)) = e^{x_t^2}(\tilde{a}(\lambda)\phi_1(\lambda, x_t) + \tilde{b}(\lambda)\phi_2(\lambda, x_t)). \quad (\text{S19})$$

This implies that  $\tilde{a} = 0$  because of the spectral equation (??), and as a nonzero Wronskian implies the independence of two solutions. Finally, we select  $\tilde{b}(\lambda)$  such that  $\langle \tilde{f}_i, \tilde{f}_j \rangle = \delta_{ij}$ ,

$$\tilde{f}(\lambda, x) = \frac{e^{x^2} \phi_2(\lambda, x)}{\langle e^{x^2} \phi_2(\lambda, x), f(\lambda, x) \rangle}. \quad (\text{S20})$$

### Appendix C: Details of the series expansion

This section repeats all results of the main text and includes detailed step by step computations. We use a shorthand notation for eigenfunctions,  $f_i(x) \equiv f(\lambda_i, x)$ . We repeat equations of the main text in order to put detailed computations in context.

We consider two leaky integrate-and-fire (LIF) model neurons receiving correlated inputs. Their dynamics are governed by the following stochastic differential equations

$$\tau_a \dot{V}_a = -V_a + \tau_a(\mu_a + \sigma_a[\sqrt{1-c} \xi_a \pm \sqrt{c} \xi_c]). \quad (\text{S21})$$

We parametrize the input  $I_a = \mu_a + \sigma_a[\sqrt{1-c} \xi_a \pm \sqrt{c} \xi_c]$ , (with index  $a = 1, 2$ ), by

$$\mu_{s,a} = J_{Ea} \nu_{s,E} - J_{Ia} \nu_{s,I} \quad (\text{S22})$$

$$\sigma_{s,a} = \sqrt{J_{Ea}^2 \nu_{s,E} + J_{Ia}^2 \nu_{s,I}} \quad (\text{S23})$$

where  $J_E$  and  $J_I$  represent the amplitude of postsynaptic potentials for excitatory and inhibitory input spike trains. We distinguish input parameters ( $J_E, J_I, \nu_E, \nu_I$ ) from intrinsic parameters ( $\tau_m, V_r, V_{th}$ ).

The corresponding Fokker-Planck equation is derived in following sections as

$$\frac{\partial P}{\partial t} = \partial_1 \left( \left( \frac{V_1}{\tau_1} - \mu_1 \right) P \right) + \partial_2 \left( \left( \frac{V_2}{\tau_2} - \mu_2 \right) P \right) + \frac{1}{2} (\partial_1 \partial_2) \begin{pmatrix} \sigma_1^2 & c\sigma_1\sigma_2 \\ c\sigma_1\sigma_2 & \sigma_2^2 \end{pmatrix} \begin{pmatrix} \partial_1 \\ \partial_2 \end{pmatrix} P \quad (\text{S24})$$

starting from the Kolmogorov Forward Equation. Here we define  $\partial_a \equiv \frac{\partial}{\partial V_a}$  and  $P \equiv P(V_1, V_2, t)$ . Using the new variables  $x = \frac{V_1 - \mu_1 \tau_1}{\sigma_1 \sqrt{\tau_1}}$  and  $y = \frac{V_2 - \mu_2 \tau_2}{\sigma_2 \sqrt{\tau_2}}$ , Eq. S24 can be rewritten as

$$\frac{\partial P}{\partial t} = \frac{1}{\tau_1} \mathcal{L}_1 P + \frac{1}{\tau_2} \mathcal{L}_2 P + \frac{c}{\sqrt{\tau_1 \tau_2}} \mathcal{L}_{12} P \quad (\text{S25})$$

$$\mathcal{L}_1 P = \frac{\partial(xP)}{\partial x} + \frac{1}{2} \frac{\partial^2 P}{\partial x^2} \quad (\text{S26})$$

$$\mathcal{L}_2 P = \frac{\partial(yP)}{\partial y} + \frac{1}{2} \frac{\partial^2 P}{\partial y^2} \quad (\text{S27})$$

$$\mathcal{L}_{12} = \frac{\partial^2 P}{\partial x \partial y}. \quad (\text{S28})$$

The first two terms represent independent populations, and they fully describe the 2D dynamics for  $c = 0$ . The third term represents the correlated diffusion for  $c > 0$ .

In order to obtain the stationary 2D membrane potential distribution we solve the steady state equation with  $\frac{\partial P}{\partial t} = 0$ ,

$$0 = \frac{1}{\tau_1} \mathcal{L}_1 P_0 + \frac{1}{\tau_2} \mathcal{L}_2 P_0 + \frac{c}{\sqrt{\tau_1 \tau_2}} \mathcal{L}_{12} P_0 \quad (\text{S29})$$

with threshold potentials  $x_t, y_t$ , reset potentials  $x_r, y_r$  and boundary conditions

$$P_0(x, y_t) = 0 = P_0(x_t, y) \quad (\text{S30a})$$

$$P_0(x, -\infty) = 0 = P_0(-\infty, y) \quad (\text{S30b})$$

$$\partial_x P_0(x_r - \epsilon, y) - \partial_x P_0(x_r + \epsilon, y) \stackrel{\epsilon \rightarrow 0}{=} \partial_x P_0(x_t, y) \quad (\text{S30c})$$

$$\partial_y P_0(x, y_r - \epsilon) - \partial_y P_0(x, y_r + \epsilon) \stackrel{\epsilon \rightarrow 0}{=} \partial_x P_0(x, y_t) \quad (\text{S30d})$$

We derive an expansion of Eq. S29 in terms of the eigenfunctions of the uncoupled operators  $\mathcal{L}_1$  and  $\mathcal{L}_2$  (index  $i$  increases with  $|\operatorname{Re}(\lambda_i)|$ )

$$\mathcal{L}_1 f_i = \lambda_{1i} f_i, \quad \mathcal{L}_2 g_i = \lambda_{2i} g_i \quad (\text{S31})$$

with boundary conditions given as

$$f_i(x_t) = 0 = \lim_{x \rightarrow -\infty} f_i(x) \quad (\text{S32})$$

$$\partial_x f_i(x_t) \stackrel{\epsilon \rightarrow 0}{=} \partial_x f_i(x_r - \epsilon) - \partial_x f_i(x_r + \epsilon). \quad (\text{S33})$$

Analogous expressions hold for  $g_i(y)$ . The eigenvalue spectrum of this equation is countable with both real and pairs of complex conjugate eigenvalues. In order to expand the solution in the eigenspace of a non-selfadjoint differential operator, the dual eigenvalue problem needs to be solved as well (derived above)

$$\mathcal{L}_1^\dagger \tilde{f}_i = \lambda_{1i} \tilde{f}_i, \quad \mathcal{L}_2^\dagger \tilde{g}_i = \lambda_{2i} \tilde{g}_i \quad (\text{S34})$$

with conjugate boundary conditions (also derived above)

$$\tilde{f}_i(x_t) = \tilde{f}_i(x_r), \quad \tilde{g}_i(y_t) = \tilde{g}_i(y_r). \quad (\text{S35})$$

In order to investigate regularized reset boundary conditions, we write derivatives of eigenfunctions in the form

$$\partial_x f_0(x) = 2r_1 \tau_1 [\kappa(x) + \sum_{k=1} X_{0k}^{(1)} f_k(x)] + A f_0(x) \quad (\text{S36a})$$

$$\partial_y g_0(y) = 2r_2 \tau_2 [\kappa(y) + \sum_{l=1} Y_{0l}^{(1)} g_l(y)] + B g_0(y) \quad (\text{S36b})$$

$$\partial_x f_i(x) = R_{1i} \kappa(x) + \sum_{k=1} X_{ik}^{(1)} f_k(x) + \frac{A}{2r_1 \tau_1} f_0(x) \quad (\text{S36c})$$

$$\partial_y g_j(y) = R_{2j} \kappa(y) + \sum_{l=1} Y_{jl}^{(1)} g_l(y) + \frac{B}{2r_2 \tau_2} g_0(y) \quad (\text{S36d})$$

where  $X^{(1)}$  are generalized Fourier coefficients of a continuous function  $\partial \bar{f}_i = \partial_x f_i - R_{1i} \kappa(x)$  and similarly for  $Y^{(1)}$ . The constants  $R$  defined above are chosen as

$$R_{1i} = -\frac{1}{2} \partial_x f_i \Big|_{x_t} = 1 \quad (\text{S37})$$

$$R_{2j} = -\frac{1}{2} \partial_y g_j \Big|_{y_t} = 1 \quad (\text{S38})$$

The box function  $\kappa$  is defined as

$$\kappa(x) = \Theta(x - x_r) - \Theta(x - x_t) \quad (\text{S39})$$

with Heaviside functions

$$\Theta(x) = \begin{cases} 0 & x \leq 0 \\ 1 & x > 0 \end{cases}.$$

It should be pointed out that one encounters an analog of the ‘‘Gibbs phenomenon’’ for generalized Fourier series for our case of a non-selfadjoint series expansion [S15]. This partially limits the convergence properties of our theory.

One can easily show via direct integration and using boundary conditions

$$\int_{-\infty}^{x_t} dx \tilde{f}_0 \partial_x f_i(x) = 0$$

$$\int_{-\infty}^{y_t} dy \tilde{g}_0 \partial_y g_i(y) = 0.$$

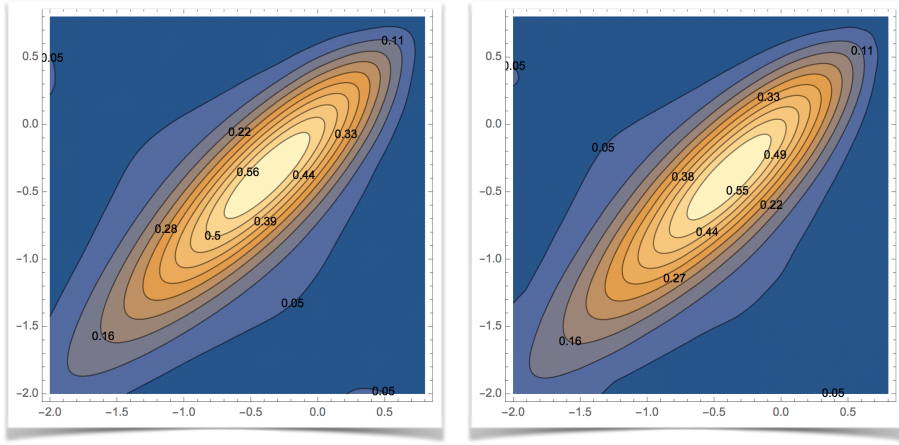


FIG. S4. Comparison of the voltage distribution from simulated data and the theoretical prediction of the 2D distribution for  $c = 0.9$ . The relative error is in the order  $10^{-2}$ . This is a quantitative demonstration of the match in Fig. 2a.

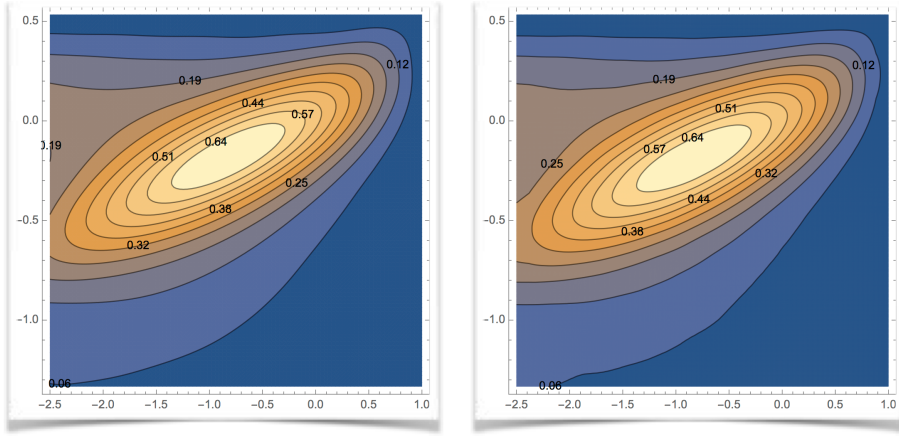


FIG. S5. Comparison of the asymmetric voltage distribution from simulated data and the theoretical prediction of the 2D distribution for  $c = 0.9$ , other parameters are as in Tab. V. The relative error is in the order  $10^{-2}$ . This is a quantitative demonstration of the match in Fig. 2a.

This implies that the projections  $\tilde{f}_0\tilde{g}_0$ ,  $\tilde{f}_0\tilde{g}_t$ ,  $\tilde{f}_k\tilde{g}_0$  are identically zero. Hence, the constants  $A$  and  $B$  are found as

$$A = - \int_{x_r}^{x_t} \tilde{f}_0 = x_r - x_t \quad (\text{S40})$$

$$B = - \int_{y_r}^{y_t} \tilde{g}_0 = y_r - y_t \quad (\text{S41})$$

The solution as a series expansion in the basis above is

$$P_0(x, y) = f_0(x)g_0(y) + F(x)SG(y) \quad (\text{S42})$$

where we define  $F(x)SG(y) = \sum_{ij} S_{ij}f_i(x)g_j(y)$ . The first column and first row of the expansion coefficients are zero except the coefficient of  $f_0g_0$ , leaving only the matrix  $S$  with  $S_{ij} \in \mathbb{C}$  as unknown. This expansion satisfies the constraints for marginal distributions

$$\int_{-\infty}^{y_t} dy P_0(x, y) = f_0(x) \int_{-\infty}^{y_t} dy g_0(y) + \sum_{ij} S_{ij}f_i(x) \int_{-\infty}^{y_t} dy g_j(y) = f_0(x) \quad (\text{S43})$$

as  $\int_{-\infty}^{y_t} dy g_0(y) = 1$  and  $\int_{-\infty}^{y_t} dy g_j(y) = 0$ . The probability distribution  $f_0(x)$  is given by

$$f_0(x) = 2r_1\tau_1 e^{-x^2} \int_x^{x_t} du \Theta(u - x_r) e^{u^2}. \quad (\text{S44})$$

A constraint for  $g_0(y)$  is given analogously. Again,  $\Theta(x)$  is the Heaviside function. Using  $\int_{-\infty}^{x_t} dx f_0(x) = 1$  and changing variables, steady state rates are given by [S5]

$$r_1 = [\sqrt{\pi}\tau_1 \int_{x_r}^{x_t} e^{u^2} (\text{erf}(u) + 1) du]^{-1}. \quad (\text{S45})$$

We obtain the same expression for  $r_2$  with the appropriate parameters. Using Eq.S31, Eq.S29 is given in terms of eigenfunctions as

$$F(x)\Lambda_1 S G(y) + F(x)S\Lambda_2 G(y) + \tilde{c}\partial_x F(x)S\partial_y G(y) = -\tilde{c}\partial_x f_0(x)\partial_y g_0(y) \quad (\text{S46})$$

with  $\Lambda_a = \frac{\lambda_{ai}}{\tau_a} \delta_{ij}$  and  $\tilde{c} = \frac{c}{\sqrt{\tau_1\tau_2}}$ . In order to solve Eq. S46 we express the action of derivative operators on the eigenbasis as

$$X_{ij} = \int_{-\infty}^{x_t} \tilde{f}_i(x) \partial_x f_j(x) dx \quad (\text{S47})$$

$$Y_{ij} = \int_{-\infty}^{y_t} \tilde{f}_i(y) \partial_y f_j(y) dy \quad (\text{S48})$$

$$X_{i0} = \int_{-\infty}^{x_t} \tilde{f}_0(x) \partial_x f_j(x) dx \quad (\text{S49})$$

$$Y_{i0} = \int_{-\infty}^{y_t} \tilde{f}_0(y) \partial_y f_j(y) dy. \quad (\text{S50})$$

The final equation in matrix form is then

$$\Lambda_1 S + S\Lambda_2 + \tilde{c}X^T S Y = -\tilde{c}X_0 \otimes Y_0. \quad (\text{S51})$$

Here we should note that we solve an equation assuming stationarity in a discrete sub-space. This is only an approximation of the unique full solution of Eq. S24. In this way, we can obtain an approximate solution (due to sub-space projections) with arbitrary precision. The way we constructed this solution provides us with explicit spike train covariance functions.

The covariance function of two stationary spike trains represented as a sum of delta functions is given as

$$C_{ij}(\tau) = \langle \sum_k \delta(t + \tau - t_k) \sum_l \delta(t - t_l) \rangle - \langle \sum_k \delta(t + \tau - t_k) \rangle \langle \sum_l \delta(t - t_l) \rangle. \quad (\text{S52})$$

It can be simplified using renewal theory in terms of the conditional rate  $r_{i|j}(\tau)$  as

$$C_{ij}(\tau) = r_i(r_{i|j}(\tau) - r_j). \quad (\text{S53})$$

For any given stationary joint membrane potential distribution  $P_0(x, y)$ , the distribution of the membrane potential conditional to spike at  $t_0 = 0$  is expressed as

$$P_{a|b}(x) = \text{Probability}(x \mid \text{spike in } [t_0, t_0 + dt]). \quad (\text{S54})$$

The conditional probability of observing a spike in the sequel is then  $P_{1|2}(x) = -\frac{1}{2r_2\tau_2}\partial_y P_0(x, y_t)$  as  $\int_{-\infty}^{x_t} dx \partial_y P_0(x, y_t) = -2r_2\tau_2$  by construction. Solving the initial value problem

$$f(t_0, x) = -\frac{1}{2r_2\tau_2}\partial_y P_0(x, y_t) \quad (\text{S55})$$

$$\partial_t f = \mathcal{L}_1 f \quad (\text{S56})$$

where  $\mathcal{L}_1$  is the time evolution operator in Eq. S31. Using  $P_0(x, y)$  the instantaneous conditional distribution is found as

$$P_{1|2}(x) = -\frac{1}{2r_2\tau_2}\partial_y P_0(x, y_t) = f_0 - \frac{1}{2r_2\tau_2} \sum_i f_i(x) \left( \sum_j S_{ij} \right), \quad (\text{S57})$$

because  $\partial_y g_0(y_t) = -2r_2\tau_2$  and  $\partial_y g_i(y_t) = -1$ . Applying the time evolution operator

$$\begin{aligned} f(x, t) &= e^{\mathcal{L}_1 t} \left[ f_0 - \frac{1}{2r_2\tau_2} \sum_i f_i(x) \left( \sum_j S_{ij} \right) \right] \\ &= f_0 - \frac{1}{2r_2\tau_2} \sum_i f_i(x) \left( \sum_j S_{ij} \right) e^{\Lambda_{1i} t} \end{aligned}$$

the conditional rate becomes

$$\begin{aligned} r_{12}(t) &= -\frac{1}{2\tau_1} \partial_x f(x_t, t) \\ &= r_1 + \frac{1}{4r_2\tau_2\tau_1} \sum_i \left( \sum_j S_{ij} \right) e^{\Lambda_{1i} t}. \end{aligned}$$

Using this in Eq. S53 yields

$$C_{12}(\tau) = r_2(r_{1|2}(\tau) - r_1) = \frac{1}{4\tau_2\tau_1} \sum_i e^{\Lambda_{1i}\tau} \left( \sum_j S_{ij} \right) \quad (\text{S58})$$

The counterpart of this is computed in a similar way

$$C_{12}(\tau) = \frac{1}{4\tau_2\tau_1} \sum_j \left( \sum_i S_{ij} \right) e^{\Lambda_{2j}\tau} \quad (\text{S59})$$

Finally, the integral of the covariance is then found as

$$\int_{-\infty}^{\infty} C(\tau) = \sum_{ij} (S\Lambda_2^{-1} + \Lambda_1^{-1}S)_{ij} \quad (\text{S60})$$

by reordering the matrices and using Eq. S51

$$\int_{-\infty}^{\infty} C(\tau) = \sum_{ij} (\Lambda_1^{-1}\Lambda_1 S\Lambda_2^{-1} + \Lambda_1^{-1}S\Lambda_2\Lambda_2^{-1})_{ij} \quad (\text{S61})$$

$$= \sum_{ij} (\Lambda_1^{-1}(-\tilde{c}XSY - \tilde{c}X_0Y_0)\Lambda_2^{-1})_{ij} \quad (\text{S62})$$

$$= -\tilde{c} \sum_{ij} (\Lambda_1^{-1}(XSY + X_0Y_0)\Lambda_2^{-1})_{ij} \quad (\text{S63})$$

### Comparison to linear response theory

The perturbative solution for small  $c$  is given as a geometric series with matrix coefficients  $S = S_0 + cS_1 + c^2S_2 + \dots$ . Inserting this into Eq. S51 we obtain

$$\tilde{c}X(S_0 + cS_1 + c^2S_2 + \dots)Y + \Lambda_1(S_0 + cS_1 + \dots) + (S_0 + cS_1 + \dots)\Lambda_2 = -\tilde{c}X_0Y_0. \quad (\text{S64})$$

We find that  $S_0 = 0$  for  $c = 0$ , since  $\Lambda_{1k}S_{0,kl} + \Lambda_{2l}S_{0,kl} = 0$  has no nonzero solution with  $\lambda_{1k} \neq -\lambda_{2k}$ , except  $\lambda_{1k} = 0 = \lambda_{2k}$  in which case we have set the coefficient of  $f_0g_0$  to 1. The  $O(c)$  equation for  $S_1$  is

$$\Lambda_1 S_1 + S_1 \Lambda_2 = -\frac{1}{\sqrt{\tau_1\tau_2}} X_0 \otimes Y_0 \quad (\text{S65})$$

and using the definition  $\psi_{kl} \equiv \frac{\sqrt{\tau_1\tau_2}}{\lambda_{1k}\tau_2 + \lambda_{2l}\tau_1}$  the solution is

$$S_{1,kl} = -\psi_{kl} X_{0,k} Y_{0,l}. \quad (\text{S66})$$

The recursion relation for terms of order  $O(c^n)$  is  $S_{n,kl} = -\psi_{kl} \sum_{ij} X_{ki} Y_{lj} S_{n-1,ij}$  with which one can expand the full perturbative series.

The result of linear response theory for output spike train correlations is given in [S6] as

$$C_{\text{out,pert}}^{(1)} = \frac{c\sigma_1\sigma_2 \frac{dr_1}{d\mu} \frac{dr_2}{d\mu}}{CV_1 CV_2 \sqrt{r_1 r_2}} = \frac{c r_1^{3/2} r_2^{3/2} [e^{x_t^2} \text{erf}(x_t) - e^{x_r^2} \text{erf}(x_r)] [e^{y_t^2} \text{erf}(y_t) - e^{y_r^2} \text{erf}(y_r)]}{CV_1 CV_2} \quad (\text{S67})$$

where  $\text{erf}(x)$  is the error function [S12]. We used the following formula for the  $CV^2 = \frac{\sigma_{ISI}^2}{\mu_{ISI}^2}$ ,

$$CV^2 = 2\pi\nu^2 \int_{y_{res}}^{y_{th}} dx e^{x^2} \int_{-\infty}^y dy [1 + \text{erf}(x)]^2 \quad (\text{S68})$$

given in [S16]. We compare this to our result (shown in Fig.4a)

$$C_{\text{out}}^{(1)} \approx -\frac{c}{4\sqrt{\tau_1\tau_2}} \sum_{ij} \left[ \Lambda_1^{-1} X_0 Y_0 \Lambda_2^{-1} \right]_{ij} + O(c^2) \quad (\text{S69})$$

and find a perfect match. Moreover,  $C_{\text{out}}$  with quadratic corrections can be easily calculated

$$C_{\text{out}}^{(2)} \approx -\frac{c}{4\sqrt{\tau_1\tau_2}} \sum_{ij} \left[ \Lambda_1^{-1} (cX X_0 \psi Y_0 Y + X_0 Y_0) \Lambda_2^{-1} \right]_{ij} + O(c^3). \quad (\text{S70})$$

where  $\psi_{kl} \equiv \frac{\sqrt{\tau_1\tau_2}}{\lambda_{1k}\tau_2 + \lambda_{2l}\tau_1}$ .

## Appendix D: 2D diffusion approximation and Fokker-Planck Equation

### 1D Fokker Planck Equation

A derivation of the Fokker-Planck equation for an Ornstein-Uhlenbeck process is given in [S17]. One starts with a 1D discrete process with PSPs given by  $\epsilon$  and  $-\epsilon$ . The excitatory and inhibitory rates are given by the formula

$$r_E = \frac{A_e}{\epsilon} + \frac{\sigma^2}{2\epsilon^2} \quad (\text{S71})$$

$$r_I = \frac{A_I}{\epsilon} + \frac{\sigma^2}{2\epsilon^2} \quad (\text{S72})$$

The “free” membrane potential takes values on a lattice  $y + k\epsilon$ , where  $y$  is resting potential. Since this defines a Markov process, the p.d.f. of transitions satisfies

$$f(x, t + \Delta t | y) = \int_{-\infty}^{\infty} f_2(x, t + \Delta t | z, t) f(z, t | y) dz \quad (\text{S73})$$

and the infinitesimal transition p.d.f. is given by

$$f_2(x, t + \Delta t | z, t) = [1 - (r_E + r_I)\Delta t] \delta(x - z) + r_E \Delta t \delta(x - z - \epsilon) + r_I \Delta t \delta(x - z + \epsilon) + o(\Delta t). \quad (\text{S74})$$

Inserting this into the integral in Eq. S73 yields

$$f(x, t + \Delta t | y) = [1 - (r_E + r_I)\Delta t] f(x, t | y) + r_E \Delta t f(x - \epsilon, t | y) + r_I \Delta t f(x + \epsilon, t | y) + o(\Delta t). \quad (\text{S75})$$

In the limit  $\Delta t \rightarrow 0$  we obtain

$$\frac{\partial}{\partial t} f(x, t + |y) = r_E [f(x - \epsilon, t | y) - f(x, t | y)] + r_I [f(x + \epsilon, t | y) - f(x, t | y)]. \quad (\text{S76})$$

Expanding right hand side into a Taylor series using

$$C_n(\epsilon) = \epsilon^n [r_E + (-1)^n r_I] \quad (\text{S77})$$

equation Eq. S76 becomes

$$\frac{\partial}{\partial t} f(x, t | y) = \sum_{n=1}^{\infty} \frac{(-1)^n}{n!} C_n \frac{\partial^n}{\partial x^n} f(x, t | y). \quad (\text{S78})$$

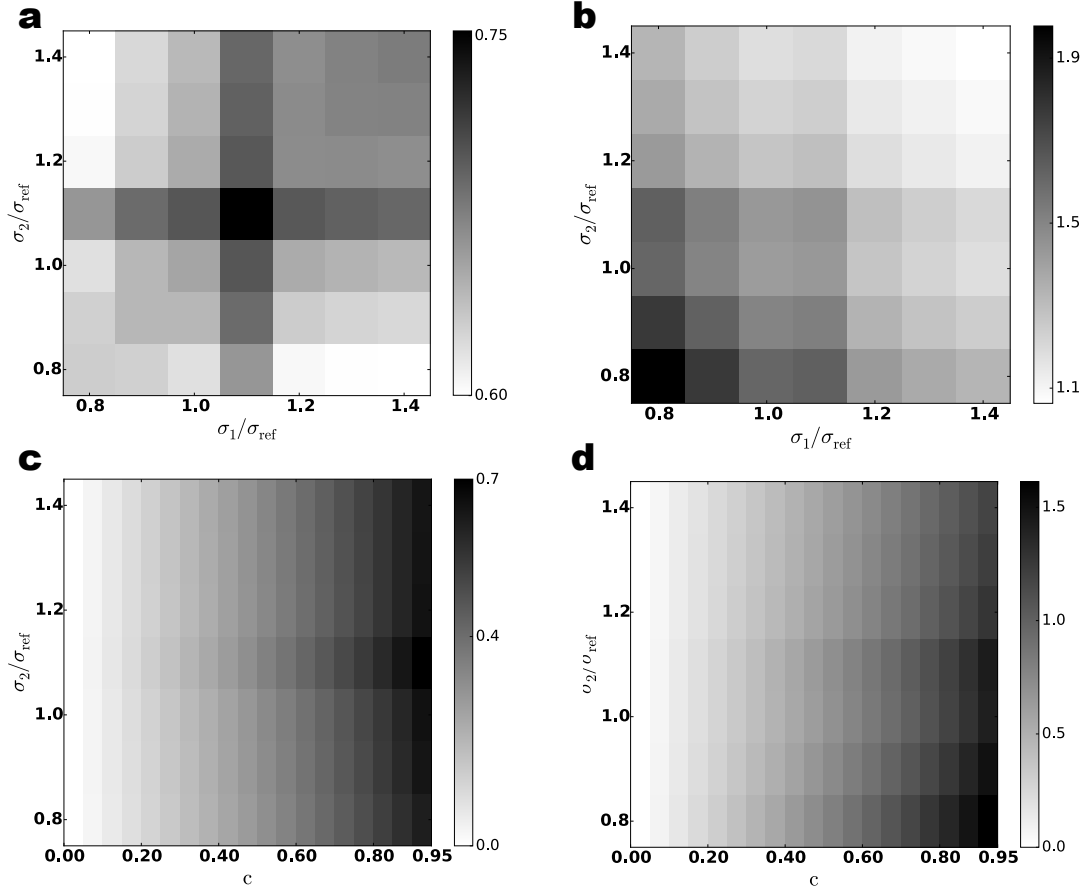


FIG. S6. Correlation and covariance transfer with respect to asymmetry of  $\sigma$ . (a) Correlation coefficient for two different input variances  $\sigma_1$  vs.  $\sigma_2$ , for  $c = 0.9$ . (b) Integral of the cross-covariance function  $\int_{-\infty}^{\infty} d\tau C_{21}(\tau)$  for two different input variances  $\sigma_1$  vs.  $\sigma_2$ , for  $c = 0.9$ . (c) Correlation coefficient for changing input variance  $\sigma_2$ , fixed  $\sigma_1 = \sigma_{ref}$  and different values of  $c$  between 0 and 0.95. (d) Integral of the cross-covariance function for changing input variance  $\sigma_2$ , fixed  $\sigma_1 = \sigma_{ref}$  and different values of  $c$  between 0 and 0.95. (See Tab. III for other parameters.)

For  $\epsilon \rightarrow 0$  all terms vanish, except the first two

$$\lim_{\epsilon \rightarrow 0} C_1(\epsilon) = \lim_{\epsilon \rightarrow 0} [\epsilon(r_E - r_I)] = A_E - A_I \equiv \mu \quad (\text{S79})$$

$$\lim_{\epsilon \rightarrow 0} C_2(\epsilon) = \lim_{\epsilon \rightarrow 0} [\epsilon^2(r_E + r_I)] = \sigma^2 \quad (\text{S80})$$

$$\lim_{\epsilon \rightarrow 0} C_{2+p}(\epsilon) = \lim_{\epsilon \rightarrow 0} [\epsilon^{(2+p)}(r_E + (-1)^{2+p}r_I)] = 0. \quad (\text{S81})$$

Hence one obtains the well-known Fokker-Planck equation as

$$\frac{\partial f}{\partial t} = -\mu \partial_x f + \frac{\sigma^2}{2} \partial_x^2 f \quad (\text{S82})$$

The generalization of this to the leaky integrate-and-fire model with time constant  $\tau$ , i.e. with an additional term of form  $\frac{-x}{\tau}$ , is straightforward. Using the definitions  $x_1 = ze^{-\Delta t/\tau}$ ,  $x_2(u) = ze^{-\Delta t/\tau} + \epsilon e^{-(t+\Delta t-u)/\tau}$ ,  $x_3(u) =$

$ze^{-\Delta t/\tau} - \epsilon e^{-(t+\Delta t-u)/\tau}$  where  $t < u < t + \Delta t$ , and then averaging over  $u$ , one obtains

$$x_1 = ze^{-\Delta t/\tau} \quad (\text{S83})$$

$$x_2 = \frac{1}{\Delta t} \int_t^{t+\Delta t} x_2(u) du = ze^{-\Delta t/\tau} + \frac{\epsilon\tau}{\Delta t} (1 - e^{-\Delta t/\tau}) \quad (\text{S84})$$

$$x_3 = \frac{1}{\Delta t} \int_t^{t+\Delta t} x_3(u) du = ze^{-\Delta t/\tau} - \frac{\epsilon\tau}{\Delta t} (1 - e^{-\Delta t/\tau}). \quad (\text{S85})$$

This leads to the infinitesimal transition p.d.f.

$$f_2(x, t + \Delta t | z, t) = [1 - (r_E + r_I)\Delta t]\delta(x_1 - x) + r_E\Delta t\delta(x_2 - x) + r_I\Delta t\delta(x_3 - x) + o(\Delta t). \quad (\text{S86})$$

Inserting this in the integral of Eq. S73 and then using  $\delta(\phi(z)) = \frac{\delta(z-\bar{z})}{|\phi'(z)|}$  (where  $\phi$  is a monotonic function which vanishes at  $\bar{z}$ ), it follows that

$$f(x, t + \Delta t | y) = e^{\Delta t/\tau} \{ [1 - (r_E + r_I)\Delta t] f(e^{\Delta t/\tau} x, t | y) + r_E\Delta t f(e^{\Delta t/\tau} x - \frac{\epsilon\tau}{\Delta t} (e^{\Delta t/\tau} - 1), t | y) + r_I\Delta t f(e^{\Delta t/\tau} x + \frac{\epsilon\tau}{\Delta t} (e^{\Delta t/\tau} - 1), t | y) \} + o(\Delta t).$$

In the limit  $\Delta t \rightarrow 0$  this becomes

$$\frac{\partial}{\partial t} f(x, t + | y) = \frac{\partial}{\partial x} \left( \frac{x}{\tau} f(x, t | y) \right) + r_E [f(x - \epsilon, t | y) - f(x, t | y)] + r_I [f(x + \epsilon, t | y) - f(x, t | y)]. \quad (\text{S87})$$

Here, drift and diffusion terms are again given as in Eq. S82. The corresponding Fokker-Planck equation is

$$\frac{\partial f}{\partial t} = \left( \frac{x}{\tau} - \mu \right) \partial_x f + \frac{\sigma^2}{2} \partial_x^2 f. \quad (\text{S88})$$

## 2D Fokker-Planck Equation

As in the 1D example above, the derivation in 2D is performed via expanding a 2D Taylor series of the right hand side of the 2D analog of Eq. S76. The three diffusion terms are  $\partial_x^2$ ,  $\partial_y^2$  and  $\partial_x \partial_y$  with corresponding diffusion constants. Concerning input spike trains, there are 6 independent sources acting in 3 directions expressed by the derivatives above. Here we assume that shared spikes can be either excitatory or inhibitory. For simplicity we assume inhibitory and excitatory PSPs have the same shape and amplitude. Following the same procedure as described above we obtain 2D infinitesimal transition probabilities as

$$\begin{aligned} P_2(x, y, t + \Delta t | z_1, z_2, t) &= \delta(y - z_2)\delta(x - z_1) + \\ &\delta(y - z_2) \{ [-(r_{1E} + r_{1I})\Delta t]\delta(x - z_1) + r_{1E}\Delta t\delta(x - z_1 - \epsilon_1) + r_{1I}\Delta t\delta(x - z_1 + \epsilon_1) \} + \\ &\delta(x - z_1) \{ [-(r_{2E} + r_{2I})\Delta t]\delta(y - z_2) + r_{2E}\Delta t\delta(y - z_2 - \epsilon_2) + r_{2I}\Delta t\delta(y - z_2 + \epsilon_2) \} + \\ &\{ [-(r_{sE} + r_{sI})\Delta t]\delta(x - z_1)\delta(y - z_2) + r_{sE}\Delta t\delta(x - z_1 - \epsilon_1)\delta(y - z_2 - \epsilon_2) + \\ &\quad + r_{sI}\Delta t\delta(x - z_1 + \epsilon_1)\delta(y - z_2 + \epsilon_2) \} + o(\Delta t). \quad (\text{S89}) \end{aligned}$$

The contribution of all lines except the last two have already been discussed for the 1D case. Here we focus on those two lines to derive the coupling term in Eq. S24. Inserting the contribution of these lines

$$\begin{aligned} &[-(r_{sE} + r_{si})\Delta t]\delta(x - z_1)\delta(y - z_2) + r_{sE}\Delta t\delta(x - z_1 - \epsilon_1)\delta(y - z_2 - \epsilon_2) \\ &\quad + r_{si}\Delta t\delta(x - z_1 + \epsilon_1)\delta(y - z_2 + \epsilon_2) \end{aligned}$$

into the 2D Kolmogorov Forward Equation (see discussion above), taking the limit  $\Delta t \rightarrow 0$  and performing Taylor expansion up to second order, is given as

$$\begin{aligned} &-(r_{sE} + r_{si})P(x, y) + r_{sE}P(x - \epsilon_1, y - \epsilon_2) + r_{si}P(x + \epsilon_1, y + \epsilon_2) = \\ &\quad - (r_{sE} - r_{sI})(\epsilon_1\partial_x P + \epsilon_2\partial_y P) + \frac{1}{2}(r_{sE} + r_{sI})(2\epsilon_1\epsilon_2\partial_1\partial_2 P + \epsilon_1^2\partial_1^2 P + \epsilon_2^2\partial_2^2 P) + o(\epsilon^2). \quad (\text{S90}) \end{aligned}$$



The simplest case for which limits  $\epsilon_1 \rightarrow 0$  and  $\epsilon_2 \rightarrow 0$  are well defined is  $\epsilon_1 = \epsilon_2 = \epsilon$ , then

$$r_{sE} = \frac{A_E}{\epsilon} + \frac{\sigma^2}{2\epsilon^2} \quad (\text{S91})$$

$$r_{sI} = \frac{A_I}{\epsilon} + \frac{\sigma^2}{2\epsilon^2}. \quad (\text{S92})$$

Reparametrizing these equations with  $c$  (as in Eq. S21), one can easily obtain the coupling terms in Eq. S24. In general we need to fix the ratio  $\frac{\epsilon_1}{\epsilon_2} = \alpha$  for the limit to converge. We now return to the parametrization with  $r$  indicating rates of input spike trains, as previously used in Eq. S22,

$$\begin{aligned} \mu_{s,a} &= J_{Ea}r_{s,E} - J_{Ia}r_{s,I} \\ \sigma_{s,a} &= \sqrt{J_{Ea}^2 r_{s,E} + J_{Ia}^2 r_{s,I}}. \end{aligned}$$

We want to emphasize that the firing rate of the shared input is independent of the neuron parameters. Here we give just a simple argument. We assume that the shared input has the property  $\mu_{s,a} = J_{Ea}r_{s,E} - J_{Ia}r_{s,I} = 0$  (balance of excitation and inhibition). This means that  $\sigma_{s,a} = \sqrt{J_{Ea}J_{Ia}r_{s,I} + J_{Ia}^2 r_{s,I}}$ . With the additional relation  $J_{Ea} = gJ_{Ia}$ , this implies that  $\sigma_{s,a} = J_{Ea}r_{s,E}$  and hence  $\frac{\sigma_{s1}}{\sigma_{s2}} = \frac{J_{E1}}{J_{E2}} = \frac{\epsilon_1}{\epsilon_2} = \alpha$  (asymmetry parameter as in Tab. II). We have the variance of the shared input and the total variance related as  $\sigma_{s,1}^2 = c\sigma_1^2$  and  $\sigma_{s,2}^2 = c\sigma_2^2$ . This means that the coupled terms (including non-diagonal terms  $\epsilon_1\epsilon_2$ ) in Eq. S97 can be expressed as

$$\frac{1}{2} (\partial_1 \ \partial_2) \begin{pmatrix} c\sigma_1^2 & c\sigma_1\sigma_2 \\ c\sigma_1\sigma_2 & c\sigma_2^2 \end{pmatrix} \begin{pmatrix} \partial_1 \\ \partial_2 \end{pmatrix} P. \quad (\text{S93})$$

Remembering that the private input variance, i.e.  $\sigma_{p,a}^2 = (1-c)\sigma_a^2$ , is a fraction of the total variance  $\sigma_a^2$ , the explicit final form amounts to

$$\begin{aligned} \frac{\partial P}{\partial t} &= \partial_1 \left( \left( \frac{V_1}{\tau_1} - \mu_1 \right) P \right) + \partial_2 \left( \left( \frac{V_2}{\tau_2} - \mu_2 \right) P \right) + \frac{1}{2} (\partial_1 \ \partial_2) \begin{pmatrix} (1-c)\sigma_1^2 & 0 \\ 0 & (1-c)\sigma_2^2 \end{pmatrix} \begin{pmatrix} \partial_1 \\ \partial_2 \end{pmatrix} P + \\ &\quad \frac{1}{2} (\partial_1 \ \partial_2) \begin{pmatrix} c\sigma_1^2 & c\sigma_1\sigma_2 \\ c\sigma_1\sigma_2 & c\sigma_2^2 \end{pmatrix} \begin{pmatrix} \partial_1 \\ \partial_2 \end{pmatrix} P. \end{aligned} \quad (\text{S94})$$

Eq. S24 follows when the two matrix terms are summed up.

Note that the most general case is a straightforward extension of the argument above. With definitions  $J_{Ea} = \epsilon_a$  and  $J_{Ia} = g_a\epsilon_a$ . We assume  $\mu_a$  and  $\sigma_a$  are finite, shared spike train rates read then

$$r_{s,E} = \frac{1}{1+g_1} \left( \frac{g_1\mu_{s1}}{\epsilon_1} + \frac{\sigma_{s1}^2}{\epsilon_1^2} \right) = \frac{1}{1+g_2} \left( \frac{g_2\mu_{s2}}{\epsilon_2} + \frac{\sigma_{s2}^2}{\epsilon_2^2} \right) \quad (\text{S95})$$

$$r_{s,I} = \frac{1}{(g_1+g_1^2)} \left( \frac{\sigma_{s1}^2}{\epsilon_1^2} - \frac{\mu_{s1}}{\epsilon_1} \right) = \frac{1}{(g_2+g_2^2)} \left( \frac{\sigma_{s2}^2}{\epsilon_2^2} - \frac{\mu_{s2}}{\epsilon_2} \right). \quad (\text{S96})$$

After simple elimination, with minimal requirements  $\frac{\sigma_{s1}}{\epsilon_1} = \frac{\sigma_{s2}}{\epsilon_2}$  and  $g_1 = g_2$ , it can be shown that  $\lim_{\epsilon \rightarrow 0} (r_{sE} + g_1g_2r_{sI})\epsilon_1\epsilon_2 = \sigma_{s1}\sigma_{s2}$  in the most general expansion

$$\begin{aligned} -(r_{sE} + r_{sI})P(x, y) + r_{sE}P(x - \epsilon_1, y - \epsilon_2) + r_{sI}P(x + g_1\epsilon_1, y + g_2\epsilon_2) = -(r_{sE} - g_1r_{sI})\epsilon_1\partial_x P - (r_{sE} - g_2r_{sI})\epsilon_2\partial_y P + \\ (r_{sE} + g_1g_2r_{sI})\epsilon_1\epsilon_2\partial_1\partial_2 P + \frac{1}{2}(r_{sE} + g_1^2r_{sI})\epsilon_1^2\partial_1^2 P + \frac{1}{2}(r_{sE} + g_2^2r_{sI})\epsilon_2^2\partial_2^2 P + o(\epsilon^2). \end{aligned} \quad (\text{S97})$$

## Appendix E: Numerical analysis and parameters

### Numerical evaluation of correlations

We compute spike train correlations via average conditional histograms. (We use `numpy.histogram()` to obtain the probability of  $P(t_i^a - t_j^b)$  using a triangular envelope around zero lag, as weight function.) One can express this

**Table 1.** Parameters for Fig. 2 and Fig. 3 of the main text

<b>Model parameters</b>		
Symbol	Description	Value
$x_t, y_t$	voltage threshold	0.8
$x_r, y_r$	voltage reset	-2.
$\tau_m$	membrane time constant	1.
<b>Simulation parameters</b>		
$dt$	time bin	0.005
$t_{\text{total}}$	total time	2000
$N_{\text{trials}}$	number of independent trials	20
<b>Data analysis parameters</b>		
$N_{\text{xbins}}$	number of bins in x diraction	300
$N_{\text{ybins}}$	number of bins in x diraction	300
$[x_-, x_t]$	data recording range	$[-3, 0.8]$
	2D boxcar smoothing range	$10 \times 10$ bins
<b>Statistics of output spike trains</b>		
$r_1, r_2$	spikes per $\tau_m$	0.231
$CV_1^2, CV_2^2$	squared coefficient of variation	0.5
<b>Numerical analysis of correlations</b>		
$T_{\text{observe}}$	observation time interval	$[-2., 2.]$
$N_{\text{bins}}$	number of bins	$\sim 450$

as an integral over two variables  $\tau = t_1 - t_2$  and  $s = t_1 + t_2$  with bin size  $\Delta$

$$C(\tau) = \frac{1}{\Delta} \int_{\tau}^{\tau+\Delta} \frac{d\tau'}{u(\tau') - l(\tau')} \int_{l(\tau')}^{u(\tau')} ds' \sum_{i,j} \delta(\tau' - \tau_i) \delta(s' - s_j) \quad (\text{S98})$$

where we have

$$u(\tau) = \begin{cases} T/\sqrt{2} - \tau & \tau < 0 \\ T/\sqrt{2} + \tau & \tau > 0 \end{cases}$$

$$l(\tau) = \begin{cases} T/\sqrt{2} + \tau & \tau < 0 \\ T/\sqrt{2} - \tau & \tau > 0 \end{cases}$$

with observation window  $T$ .

### Solution of stochastic differential equations

We used Euler-Maruyama scheme to integrate stochastic differential equations, like the Ornstein-Uhlenbeck Process

$$\tau \dot{V} = -V + \mu + \sigma \sqrt{\tau} [\sqrt{1-c} \xi \pm \sqrt{c} \xi_c]. \quad (\text{S99})$$

The discrete time approximation with  $t_0 < t_1 < t_2 \dots < t_n < T$  is then

$$V_{i+1} = \left(1 - \frac{dt}{\tau}\right) V_i + \frac{dt}{\tau} \mu + \sqrt{\frac{dt}{\tau}} [\sqrt{1-c} n_i \pm \sqrt{c} n_{c,i}] \quad (\text{S100})$$

where  $n_i$  and  $n_{c,i}$  are normally distributed random numbers  $\sim \mathcal{N}(0, 1)$ .

### Voltage data and smoothing

We simulated the stochastic differential equation in `Python`. We recorded simulated data for several trials and binned 2D data with the function `numpy.histogram()`. We averaged the histogram for  $N_{\text{trial}}$  trials. We smoothed the histogram data with a 2D boxcar kernel averaging over  $m \times n$  bins. Parameters used are given in Tab. I.

**Table 2.** Parameters for Fig. 4a of the main text

<b>Numerical analysis data</b>		
Symbol	Description	Value
$C_{in}$	range of input correlation data points	[0, 0.95]
$\Delta C_{in}$	step of input correlation data points	0.05
<b>Model 1 (dark blue) parameters</b>		
$x_t, y_t$	voltage threshold	0.8
$x_r, y_r$	voltage reset	-2.
$\tau_m$	membrane time constant	1.
<b>Statistics of output spike trains 1</b>		
$r_1, r_2$	spikes per $\tau_m$	0.231
$CV_1^2, CV_2^2$	squared coefficient of variation	0.5
<b>Model 2 (dark green) parameters</b>		
$x_t, y_t$	voltage threshold	2.
$x_r, y_r$	voltage reset	-1.
$\tau_m$	membrane time constant	1.
<b>Statistics of output spike trains 2</b>		
$r_1, r_2$	spikes per $\tau_m$	0.017
$CV_1^2, CV_2^2$	squared coefficient of variation	0.98

**Table 3.** Parameters for Fig. 4b, Fig. 4c of the main text

<b>Neuron 1 parameters</b>		
Symbol	Description	Value
$x_t$	voltage threshold	in [1., 0.5]
$x_r$	voltage reset	in [-2.5, -1.25]
$\tau_m$	membrane time constant	1.
<b>Neuron 2 parameters</b>		
$y_t$	voltage threshold	in [1., 0.5]
$y_r$	voltage reset	in [-2.5, -1.25]
$\tau_m$	membrane time constant	1.
<b>Reference parameters and sigma asymmetry</b>		
$x_{t,ref}$	voltage threshold	0.8
$x_{r,ref}$	voltage reset	-2.
$\tau_m$	membrane time constant	1.
	data points for $x = \frac{V - \mu\tau}{\alpha\sigma\sqrt{\tau_m}}$	$\alpha$ in [0.8, 1.5] with steps of 0.1
<b><math>\sigma/\sigma_{ref}</math> vs <math>C_{out}</math></b>		
$C_{in}$	range of input correlation data points	[0, 0.95]
$\Delta C_{in}$	step of input correlation data points	0.05

**Table 4.** Parameters for Fig. 4d of the main text

<b>Neuron 1 parameters</b>		
Symbol	Description	Value
$x_t$	voltage threshold	0
$x_r$	voltage reset	-2.5
$\tau_m$	membrane time constant	1.
<b>Neuron 2 parameters</b>		
$y_t$	voltage threshold	0.83
$y_r$	voltage reset	-1.66
$\tau_m$	membrane time constant	1.
<b>Input correlations</b>		
$C_{in}$	input correlation	0.9

**Table 5.** Parameters for Fig. 4e of the main text

<b>Neuron 1 parameters</b>		
Symbol	Description	Value
$x_t$	voltage threshold	1.
$x_r$	voltage reset	-2.5
$\tau_m$	membrane time constant	1.5
<b>Neuron 2 parameters</b>		
$y_t$	voltage threshold	0.5
$y_r$	voltage reset	-1.25
$\tau_m$	membrane time constant	1.
<b>Input correlations</b>		
$C_{in}$	input correlation	0.9

- 
- [S5] N. Brunel and V. Hakim, *Neural Computation* **11**, 1621 (1999), arXiv:9904278 [cond-mat]; B. Lindner and L. Schimansky-Geier, *Physical Review Letters* **86**, 2934 (2001).
- [S6] J. de la Rocha, B. Doiron, E. Shea-Brown, K. Josić, and A. Reyes, *Nature* **448**, 802 (2007); E. Shea-Brown, K. Josić, J. de la Rocha, and B. Doiron, *Physical Review Letters* **100**, 108102 (2008).
- [S12] M. Abramowitz, *Handbook of Mathematical Functions, With Formulas, Graphs, and Mathematical Tables*, (Dover Publications, Incorporated, 1974).
- [S13] S. Ostojic, *Journal of neurophysiology* **106**, 361 (2011).
- [S14] H. Risken, *The Fokker-Planck Equation: Methods of Solutions and Applications, 2nd ed.* (Springer Verlag, Berlin, Heidelberg, 1996).
- [S15] B. Adcock and A. C. Hansen, *Applied and Computational Harmonic Analysis* **32**, 357 (2012), arXiv:arXiv:1011.6625v1.
- [S16] N. Brunel, *Neurocomputing* **32-33**, 307 (2000).
- [S17] S. S. Luigi M. Ricciardi, *Journal of Applied Probability* **25**, 43 (1988)